Contribution from the Departments of Chemistry, State University of New York at Albany, Albany, New York 12222, and University of Virginia, Charlottesville, Virginia 22901

Models for Met-Hemocyanin Derivatives: Structural and Spectroscopic Comparisons of Analogous Phenolate and X (X = OH^-, OMe^-, N_3^-, Cl^-, OAc^-, OBz^-) Doubly Bridged Dinuclear Copper(II) Complexes

Kenneth D. Karlin,*† Amjad Farooq,† Jon C. Hayes,† Brett I. Cohen,† Theresa M. Rowe,‡ Ekkehard Sinn,*‡ and Jon Zubieta*†

Received June 6, 1986

The extensive use of spectroscopic and chemical studies of the binding of small molecules such as acetate, chloride, azide, etc. in chemically modified hemocyanin derivatives has prompted us to develop the chemistry of the dinucleating ligand L-OH, which can be utilized to form the compounds $[Cu_2(L\text{-}O^-)X]^{2+}$, where two copper(II) ions are bridged by a phenolate oxygen atom from $L\text{-}O^-$ and the exogenous X^- bridging atom. Here, we report structural, magnetic, and spectroscopic comparisons for a series of complexes, X = OH^- (I^{2+}), OMe^- (IV^{2+}), N_3^- (II^{2+}), Cl^- (III^{2+}), Br^- (V^{2+}), OBz^- (VI^{2+}), OAc^- (VII^{2+}), including complete X-ray structural characterization of complexes III, IV, and V. Compound III crystallizes in the triclinic space group $P\bar{1}$ with $Z = 2$ and $a = 10.986$ (3) Å, $b = 15.138$ (3) Å, $c = 23.292$ Å, $\alpha = 91.11$ (2)°, $\beta = 99.77$ (2)°, and $\gamma = 91.18$ (2)°. Complex IV crystallizes in the triclinic space group $P\bar{1}$ with $Z = 2$ and $a = 10.843$ (2) Å, $b = 15.045$ (3) Å, $c = 23.170$ (4) Å, $\alpha = 90.14$ (2)°, $\beta = 100.29$ (2)°, and $\gamma = 96.27$ (2)°. Compound V crystallizes in the monoclinic space group $C2/c$ with $Z = 4$ and $a = 15.740$ (4) Å, $b = 32.033$ (4) Å, $c = 13.033$ (4) Å, and $\beta = 134.03$ (2)°. In these complexes, each copper atom is coordinated in a square-based pyramidal (SP) or distorted SP geometry to three nitrogen atoms provided by $L\text{-}O^-$, the bridging phenolate oxygen atom, and X. Structural comparisons are made among compounds I–V; the presence of a larger X atom results in a distortion away from pure SP geometry with an opening of the Cu1–O1–Cu2 bridging angle resulting in a greater Cu···Cu separation. UV–vis spectroscopic comparisons indicate that the $OPh^- \rightarrow Cu(II)$ LMCT transition (λ_{max} = 378–475 nm) and the d–d envelope (λ_{max} = 625–680 nm) vary systematically with structure; a shift to lower energy is observed for both types of electronic absorption as X becomes larger. On the basis of these and other observations, complexes VI and VII are assigned a monoatomic μ-carboxylato-$O(O')$ structure in solution, but a μ-carboxylato-O,O' coordination in the solid state. Temperature-dependent magnetic measurements on the structurally characterized complexes I–III and V reveal that the halide-bridged complexes are the least strongly coupled with singlet–triplet separations, $-2J$, of 335 cm^{-1} for each. The OH^- complex is the most strongly coupled of the series ($-2J$ = 600 cm^{-1}), while the azide complex falls in between ($-2J$ = 440 cm^{-1}). On the basis of only the $Cu\text{–}O_{phenolate}\text{–}Cu$ angles, the coupling should increase in the direction $OH^- < \mu\text{-}1,1\text{-}N_3^- < Br^-$, but the opposite trend is actually observed and is attributed to the modulating effect of the exogenous bridge.

Introduction

Studies aimed at the elucidation of the structure, physical properties, and reactivity of the active site in proteins containing dinuclear copper active sites have recently attracted a great deal of attention.[1] Hemocyanin and tyrosinase both contain antiferromagnetically coupled dinuclear active sites which interact with molecular oxygen as part of their biological function. Hemocyanin functions as a reversible dioxygen carrier in several arthropods and molluscs, binding one dioxygen molecule as peroxide to the dinuclear copper active site. Tyrosinase is a monooxygenase that utilizes dioxygen in the hydroxylation of monophenols to diphenols, further acting as a two-electron oxidase in the oxidation of *o*-diphenols to *o*-quinones.

A detailed picture of the active sites has emerged as a result of the experiments that have relied on spectroscopic investigations of the proteins and protein derivatives.[1,2] Studies of several protein derivatives have revealed the following: (i) The active sites contain two antiferromagnetically coupled Cu(II) ions. (ii) The two Cu(II) atoms in the oxygenated proteins are in an approximate tetragonal geometry with a $d_{x^2-y^2}$ ground state. (iii) The ligand L (CH_3COO^-, NO_2^-, F^- Cl^-, Br^-, I^-, SCN^-, CN^- or N_3^-) in the "met-apo",[5] "half-met",[5] "met", and "dimer" derivatives coordinates in the

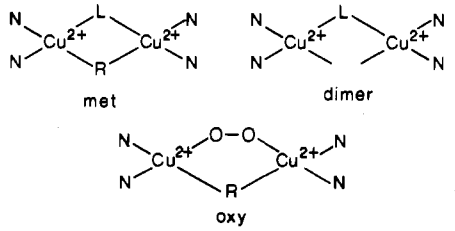

equatorial plane of the tetragonal copper site. (iv) Dioxygen binds as a peroxide in the equatorial plane of the oxy derivatives. (v) Exogenous ligands, L, bridge the two copper atoms in the "half-met" sites. This suggests that the peroxide moiety bridges the coppers in the oxy derivatives. (vi) An endogenous group R is thought to bridge the two copper atoms in the "oxy", "met", and "half-met" derivatives, where R is an oxygen atom donor that may be from tyrosine or serine or from a coordinated water or hydroxide ligand.[6]

Interest in copper proteins possessing dinuclear centers and their met derivatives has prompted us and others to study model systems that employ dinucleating ligands. In this paper, we amplify upon our previous communications,[11-14] which described the doubly

†State University of New York at Albany.
‡University of Virgina.

(1) Solomon, E. I.; Penfield, K. W.; Wilcox, D. E. *Struct. Bonding (Berlin)* **1983**, *53*, 1–57.
(2) Solomon, E. I. In *Copper Proteins*; Spiro, T. G., Ed.; Wiley: New York, 1981; Vol. 3, pp 41–108.
(3) *Copper Coordination Chemistry: Biochemical & Inorganic Perspectives*; Karlin, K. D., Zubieta, J., Eds.; Adenine: Guilderland, NY, 1983.
(4) *Biological and Inorganic Copper Chemistry*; Karlin, K. D., Zubieta, J., Eds.; Adenine: Guilderland, NY, 1986; Vols. 1 and 2.
(5) "met-apo" is the protein derivative with only one copper site occupied and the other with Cu^{2+}, while "half-met" derivatives are mixed-valence species, i.e. $Cu^+\cdots Cu^{2+}$.[1,2]
(6) A recent crystal structure of deoxy-hemocyanin[7] indicates that three imidazole ligands are coordinated to each Cu(I) ion (Cu···Cu = 3.8 ± 0.4 Å). This, along with sequence homology studies of various hemocyanins,[8] suggests that tyrosine is unlikely to be a ligand for copper in oxy or met forms of hemocyanin. While there exists some evidence for an endogenous bridging ligand in met-hemocyanin derivatives,[9] the situation is less clear for oxy-hemocyanin.[10]
(7) Gaykema, W. P. J.; Hol, W. G. J.; Verijken, J. M.; Soeter, M. M.; Bok, H. J.; Beintema, J. J. *Nature (London)* **1984**, *309*, 23–29.
(8) Linzen, B.; Soeter, N. M.; Riggs, A. F.; Schneider, H. J.; Schartav, W.; Moore, M. D.; Yokota, E.; Behrens, P. Q.; Nakashima, H.; Takagi, T.; Nemoto, T.; Vereijken, J. M.; Bok, H. J.; Beintema, J. J.; Volbeda, A.; Gaykema, W. P. J.; Hol, W. G. J. *Science (Washington, D.C.)* **1985**, *229*, 519–524.
(9) Wilcox, D. E.; Long, J. R.; Solomon, E. I. *J. Am. Chem. Soc.* **1984**, *106*, 2186–2194.
(10) Karlin, K. D.; Haka, M. S.; Cruse, R. W.; Gultneh, Y. *J. Am. Chem. Soc.* **1985**, *107*, 5828.
(11) Karlin, K. D.; Hayes, J. C.; Gultneh, Y.; Cruse, R. W.; McKown, J. W.; Hutchinson, J. P.; Zubieta, J. *J. Am. Chem. Soc.* **1984**, *106*, 2121–2128.

0020-1669/87/1326-1271$01.50/0

bridged cupric compounds with the ligand L-O$^-$ and the exogenous bridging atoms OH$^-$,[11] OMe$^-$,[15] N_3^-,[12-14] Cl$^-$.[12] We have already reported the synthesis and characterization of the phenolate-bridged, tetragonally coordinated, dinuclear Cu(II) complexes I[11] and IV,[15] which have been characterized by X-ray diffraction. Here, we also report the synthesis and characterization of complexes in which bromide, acetate, and benzoate are introduced to serve as exogenous bridging ligands. The doubly bridged

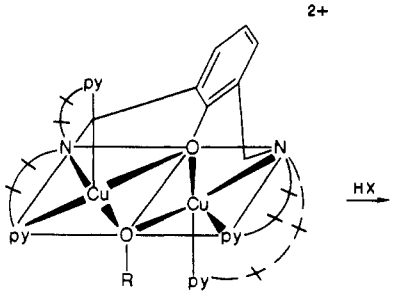

$[Cu_2(L\text{-}O^-)OR]^{2+}$

R = H (I^{2+}), Me (IV^{2+})

py = 2-pyridyl

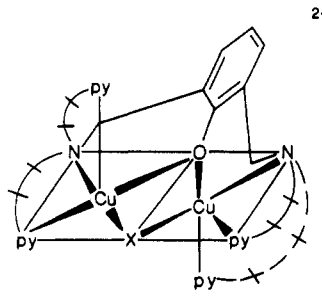

$[Cu_2(L\text{-}O^-)X]^{2+}$

X = N_3^- (II^{2+}), Cl (III^{2+}), Br$^-$ (V^{2+}), OBz$^-$ (VI^{2+}), OAc$^-$ (VII^{2+})

dinuclear cupric complexes are studied in order to gain information about the effect that a specific exogenous bridging group has on the physicochemical properties such as the cupric coordination geometry, copper–copper separation and bridging geometry, and spectral and magnetic properties.

Experimental Section

Materials and Methods. Reagents and solvents used were of commercially available reagent grade quality. Methanol was distilled from $Mg(OMe)_2$, acetone from anhydrous K_2CO_3, and dichloromethane from CaH_2–K_2CO_3, all under argon. Dimethylformamide (DMF) was used from freshly opened bottles (glass distilled, MCB Omnisolv) and/or stored over 4-Å molecular sieves. Elemental analyses were performed by Galbraith Laboratories, Inc., Knoxville, TN, or Mic Anal, Tucson, AZ. Infrared and electronic absorption spectra were taken with PE283 and Varian DMS90 instruments, respectively. Electrical conductivity measurements were carried out in DMF with an Industrial Instruments Inc. conductivity bridge. The cell constant was determined by using a standard aqueous solution of KCl. The EPR spectra of frozen solutions of complexes I–VII (except complex IV) in DMF–$CHCl_3$ (1:1) were obtained with a Varian E-4 spectrometer equipped with a liquid-nitrogen Dewar insert. The EPR spectra were obtained at 77 K, and calibration was effected by using diphenylpicrylhydrazyl (DPPH). The room-temperature magnetic susceptibility for compound VII was recorded with a Johnson Matthey magnetometer. The instrument was calibrated by using $Hg[Co(SCN)_4]$.

Compound Synthesis. $[Cu_2(L\text{-}O^-)Cl][BPh_4]_2\cdot CH_3COCH_3$ (III). Compound I[11] (1.0 g, 9.95×10^{-4} mol) was dissolved in 130 mL of acetone to yield a green solution. Dimethoxypropane (2–3 mL) was then added to the solution followed by the dropwise addition of 10.5 mL of a 0.1 M aqueous HCl solution. Addition of the acid resulted in the immediate formation of a dark brown solution. An acetone solution of sodium tetraphenylborate (0.95 g, 0.028 mol) was then added to the copper solution. The resulting solution was stirred before layering with dry diethyl ether. A yield of 1.3 g (96%) of compound III was obtained. Anal. Calcd for $C_{87}H_{85}N_6B_2ClO_2Cu_2$: C, 73.03; H, 5.98; N, 5.87; Cl, 2.48. Found: C, 72.88; H, 6.15; N, 5.82; Cl, 2.19. Molar conductivity: Λ_m = 95.0 Ω^{-1} cm^2 mol^{-1}.

$[Cu_2(L\text{-}O^-)CH_3O][BPh_4]_2$ (IV). $[Cu_2(m\text{-xylpy2})](PF_6)_2$[11] (*m*-XYLpy2 = 1,3-bis(bis(2-(2-pyridyl)ethyl)amino)methyl)benzene) (0.4 g, 4.1×10^{-4} mol) was dissolved in 10 mL of dichloromethane, under argon. The solution was then exposed to dry oxygen and stirred for 2 h. The resulting green solution was concentrated and washed with dichloromethane to yield a green solution and a blue-green precipitate. The dichloromethane-insoluble material was dissolved in 50 mL of methanol, and the solution was filtered. The filtrate was precipitated out with excess diethyl ether, and 0.1 g of the precipitate obtained was redissolved in 40 mL of methanol, under argon. To this solution was added 0.1 g (2.92×10^{-4} mol) of sodium tetraphenylborate in 50 mL of methanol under argon. The solution immediately turned light yellow. Exposure of this solution to dioxygen resulted in a green solution, from which a green precipitate was obtained upon addition of diethyl ether. Green cubic-shaped crystals of IV were obtained from vapor diffusion of methanol into a DMF solution of the complex. molar conductivity: Λ_m = 90.0 Ω^{-1} cm^2 mol^{-1}.

$[Cu_2(L\text{-}O^-)Br][PF_6]_2\cdot 0.5CH_2Cl_2$ (V). Compound I[11] (1.50 g, 1.49×10^{-3} mol) was dissolved in 115 mL of dry dichloromethane to which 0.503 g of 48.0% aqueous HBr (2.98×10^{-3} mol) was added dropwise. Addition of the acid resulted in the formation of a reddish brown solution in about 30 min, and the resulting solution was stirred for 12 h. Molecular sieves (type 4A, 8–12 mesh beads, MCB) were put into the stirring solution and were kept there for 4 h. The solution was then filtered. Diethyl ether was layered on the solution to yield 0.940 g (51% yield) of crystals of compound V. Anal. Calcd for $C_{36.5}H_{40}N_6BrF_{12}ClP_2OCu_2$: C, 39.44; H, 3.60; N, 7.56. Found: C, 40.08; H, 3.60; N, 7.81. Molar conductivity: Λ_m = 102 Ω^{-1} cm^2 mol^{-1}.

$[Cu_2(L\text{-}O^-)C_6H_5COO][PF_6]_2\cdot CH_2Cl_2$ (VI). To a solution of a 1.50 g of compound I[11] (1.49×10^{-3} mol) in 100 mL of dry CH_2Cl_2, with stirring, was added dropwise 0.300 g (2.46×10^{-3} mol) of benzoic acid in 25 mL of dry CH_2Cl_2. The resulting solution was stirred for 2 days. Molecular sieves (type 4A, 8–12 mesh beads, MCB) were put into the brown solution and were kept there for 2 h. The mixture was filtered under argon, and diethyl ether was layered on the solution, which yielded a mixture of green crystals and brown powder. Removal of the solvent by evacuation gave a brown powder, which was recrystallized from dichloromethane–ether to give 1.08 g (9.04×10^{-4} mol, 65% yield) of compound VI. Anal. Calcd for $C_{44}H_{47}N_6F_{12}Cl_2P_2O_3Cu_2$: C, 44.20; H, 3.940; N, 7.03. Found: C, 44.54; H, 3.92; N, 7.46. Molar conductivity: Λ_m = 137 Ω^{-1} cm^2 mol^{-1}.

$[Cu_2(L\text{-}O^-)CH_3COO][PF_6]_2\cdot CH_2Cl_2$ (VII). To a solution of 0.500 g of compound I[11] (4.98×10^{-4} mol) in 50 mL of dry CH_2Cl_2, with stirring, was added dropwise 0.0597 g (9.95×10^{-4} mol) of acetic acid in 10 mL of dry CH_2Cl_2. This solution was stirred overnight. Molecular sieves (type 4A, 8–12 mesh beads, MCB) were put into the brown solution and were kept there for 2 h. The mixture was filtered under argon. After diffusion of diethyl ether, which had been layered on the solution, thin rectangular-shaped brown crystals were obtained. These crystals were washed with dry ether and dried under vacuum, whereupon recrystallization from dichloromethane–ether gave 0.15 g (1.43×10^{-4} mol, 26.6% yield) of compound VII. Anal. Calcd for $C_{39}H_{44}N_6F_{12}P_2O_3Cu_2Cl_2$: C, 41.34; H, 3.89; N, 7.42. Found: C, 41.54; H, 3.89; N, 7.47. Molar conductivity Λ_m = 124 Ω^{-1} cm^2 mol^{-1}.

Magnetism. Magnetic susceptibilities were determined down to 10 K on a cryostat-controlled SQUID magnetometer. The calibration and method of operation were as described previously.[35] The data were fitted to the dinuclear model

$$\chi = \frac{Ng^2\beta^2}{kT}\left[\frac{1-P}{3+e^{-2J/kT}} + \frac{-P}{4}\right]$$

where $100P$ is the percentage of paramagnetic impurity, g is the Lande g factor, and J gives the strength of coupling, based on the Hamiltonian $H = -2JS_1\cdot S_2$. For strong antiferromagnetic coupling, the effect on χ of a small paramagnetic impurity is significant only at the lowest temperatures, making it essentially independent of the contribution by the dinuclear complex, which is only seen at high temperatures. The equation therefore allows accurate determination of J. The less important (here) g values are always less accurate (g_{calcd} = 2.0 for I, 2.10 for II, and 2.15 for III and V) because these are multipliers of the entire set of data and

(12) Karlin, K. D.; Hayes, J. C.; Hutchinson, J. P.; Zubieta, J. *J. Chem. Soc., Chem. Commun.* **1983**, 376–378.
(13) Karlin, K. D.; Cohen, B. I. *Inorg. Chim. Acta* **1985**, *107*, L17–L20.
(14) Karlin, K. D.; Cohen, B. I.; Hayes, J. C.; Farooq, A.; Zubieta, J. *Inorg. Chem.* **1987**, *26*, 147–153.
(15) Karlin, K. D.; Dahlstrom, P. L.; Cozzette, S. N.; Scensny, P. M.; Zubieta, J. *J. Chem. Soc., Chem. Commun.* **1981**, 881–882.

Table I. Crystallographic Data for Complexes III–V

	III, X = Cl^-	IV, X = OCH_3^-	V, X = Br^-
Crystal Data			
temp, K	294	294	294
a, Å	10.986 (3)	10.843 (2)	15.740 (4)
b, Å	15.138 (3)	15.045 (3)	32.033 (4)
c, Å	23.292 (5)	23.170 (4)	13.033 (4)
α, deg	91.11 (2)	90.14 (2)	90.00
β, deg	99.77 (2)	100.29 (2)	134.03 (2)
γ, deg	96.18 (2)	96.27 (2)	90.00
V, Å^3	3792.4	3695.4	4806.03
F(000)	1500	1436	2312
Z	2	2	4
D_{calcd}, g/cm^3	1.25	1.23	1.53
space group	$P\bar{1}$	$P\bar{1}$	$C2/c$
cryst dimens, mm	0.15 × 0.18 × 0.16	0.12 × 0.20 × 0.14	0.10 × 0.15 × 0.10
scan rate, deg/min	8.0–30.0	7.0–30.0	7.0–30.0
scan range, deg	3.0–45.0	3.0–30.0	3.0–40.0
bkdg measurement	stationary cryst, stationary counter, at the beginning and end of each 2θ scan, each for the time taken for the scan		
reflecns measd	$+h,\pm k,\pm l$	$+h,\pm k,\pm l$	$\pm h,+k,+l$
reflecns collected	10786	3316	4987
indep reflecns	4669 ($\geq 6\sigma\|F_o\|$)	1566 ($\geq 6\sigma\|F_o\|$)	1029 ($\geq 4\sigma\|F_o\|$)
abs coeff, cm^{-1}	6.70	6.50	19.69
Reduction of Intensity Data and Summary of Structure Solution and Refinement[a]			
agreement between equiv reflecns	0.021	0.020	0.020
abs cor	not applied	not applied	not applied
atom scattering factors[b]	neutral atomic scattering factors used throughout anal.		
anomalous dispersion[c]	applied to all non-hydrogen atoms		
R[d]	0.0802	0.0807	0.1016
R_w[d]	0.0809	0.0804	0.0997
goodness of fit[e]	1.903	2.871	2.092

[a] Data were corrected for background, attenuators, Lorentz, and polarization effects in the usual fashion: Hyde, J.; Venkatasubramanian, K.; Zubieta, *J. Inorg. Chem.* **1978**, *17*, 414. [b] Cromer, D. T.; Mann, J. B. *Acta Crystallogr., Sect. A: Cryst. Phys., Diffr., Theor. Gen. Crystallogr.* **1968**, *24*, 321. [c] *International Tables for X-ray Crystallography*; Kynoch: Birmingham, England, 1962; Vol. III. [d] $R = \sum[|F_o| - |F_c|/\sum|F_o|]$; $R_w = [\sum w(|F_o| - |F_c|)^2/\sum w|F_o|^2]^{1/2}$; $w = 1/\delta^2(F_o) + g^*(F_o)^2$; $g = 0.001$. [e] GOF $= [\sum w(|F_o| - |F_c|)^2/(NO - NV)]^{1/2}$, where NO is the number of observations and NV is the number of variables.

are essentially independent of the temperature behavior of the magnetism; weighing and calibration errors and the presence of diamagnetic impurities such as solvent would all show up as an effect on the g value alone. Experimental plots of μ_{eff} and χ vs. $T(k)$ for compounds I–III and V are provided as supplementary material.

X-ray Crystallography. Crystallization, Data Collection, and Reduction. Brown crystals of compound III suitable for X-ray crystallographic analysis were obtained from an acetone–diethyl ether solution. Green cubic-shaped X-ray-quality crystals of the compound IV were obtained from vapor diffusion of methanol into a DMF solution. Reddish brown crystals of compound V, suitable for X-ray diffraction analysis, were obtained from a dichloromethane–diethyl ether solution. Epoxy-covered crystals of compounds III–V were mounted on a Nicolet R 3m four-circle automated diffractometer with a Mo X-ray source equipped with a highly ordered graphite monochromator (λ(Mo Kα) = 0.71073 Å). Automatic centering and least-squares routines were carried out on 25 reflections for compound IV, 24 reflections for compound III, and 16 reflections for compound V to obtain the unit cell parameters and Bravais lattice type that are given in Table I. A coupled θ(crystal)–2θ(counter) scan mode was employed. The scan length was $(2\theta(K\alpha_1 - 1.0))°$ to $(2\theta(K\alpha_2 + 1.0))°$. Three check reflections were measured every 197 reflections; these exhibited no significant decay during data collection.

The program XTAPE of the SHELXTL package[16] was used to process the data for complexes III–V. A summary of cell parameters, data collection parameters, and refinement results for complexes II–V is found in Table I.

Structure Solution and Refinement. In each case, the positional parameters of the copper atoms were determined by the Patterson method. The remaining non-hydrogen atoms were located by subsequent difference Fourier maps and least-squares refinements. Atomic scattering factors for neutral atoms were used throughout the analysis. The tetraphenylborate salt of compound III crystallizes in the triclinic space group $P\bar{1}$, with two molecules in each unit cell. Complex IV also crystallizes in the triclinic space group $P\bar{1}$ with $Z = 2$. Complex V crystallizes in the monoclinic space group $C2/c$, with four molecules in the unit cell. For complex III, all of the non-hydrogen atoms in the cation and the boron atoms from the anions were refined anisotropically. The remaining non-hydrogen atoms were refined isotropically. For complex IV, only copper atoms were refined anisotropically. All of the remaining atoms were refined with isotropic thermal parameters. For complex V, copper, bromide, and the phenoxo oxygen were refined anisotropically. All remaining non-hydrogen atoms were refined isotropically. For compexes III and IV, the hydrogen atoms on both the cations and the anions were included in the final stages of refinement. For complex V, the hydrogen atoms were included in the final stages of refinement for the complex cation. The carbon–hydrogen bond lengths were set at 0.96 Å, and isotropic thermal parameters were 1.2 times those of the bonded carbon atoms. The two tetraphenylborate anions for complex IV were unexceptional with no unusual bond distances or angles. For complex V, two hexafluorophosphate anions were located. Each had occupancy factors of 0.5. One was not disordered, and its bonding parameters were as expected. The other anion was found to be disordered. Four fluorine fragments were located. When added together, they accounted for all the expected fluorine electron density for this molecule. Solvents of crystallization, identified as acetone for complex III and dichloromethane with an occupancy factor of 0.478 for complex V, were located in the final stages of refinement. The final R factors and refinement data appear in Table I.

Structure factors, bond lengths, bond angles, anisotropic temperature factors, and hydrogen coordinates and temperature factors are available in the supplementary material for compounds III (Tables X–XIV), IV (Tables XV–XIX), and V (Tables XX–XXIV).

Discussion

Synthesis. We recently reported the synthesis and characterization of a dinuclear copper complex containing three-coordinate Cu(I) ions with amino and pyridine nitrogen donor atoms. Addition of dioxygen to this complex results in the hydroxylation of the *m*-xylyl dinucleating ligand, producing the phenolate-bridged tetragonally coordinated dinuclear Cu(II) complexes I and/or IV.[11]

The X-bridged derivatives II, III, and V–VII are easily prepared by the addition of HX (X = azide, chloride, bromide, benzoate, acetate) to a solution of I, followed by precipitation with diethyl

(16) All calculations were performed on a Data General Nova 3 computer with 32K of 16-bit words using local versions of the Nicolet SHELXTL interactive crystallographic software package, as described in: Sheldrick, G. M. *Nicolet SHELXTL Operations Manual*; Nicolet XRD Corp.: Cupertino, CA, 1979.

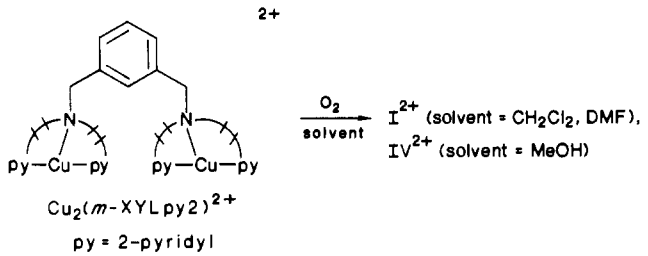

ether and recrystallization. NaX can also be utilized in these substitution reactions. The methoxide complex IV is more difficult to prepare in reasonable quantities, since the major product of the hydroxylation reaction in methanol is I. As indicated in the Experimental Section, IV can also be isolated via a circuitous route in which tetraphenylborate anion in methanol is used to reduce a Cu(II) species containing *m*-XYLpy2, followed by exposure to air and hydroxylation, giving small yields of IV. All of the X-bridged derivatives, II–VII, must be handled in the absence of moisture since they readily convert to the thermodynamically more stable hydroxo-bridged complex I.

Description of Structures. $[Cu_2(L\text{-}O^-)Cl]^{2+}$ (III^{2+}). Final positional parameters are given in Table V, and selected bond distances and angles are found in Table II. An ORTEP view of $[Cu_2(L\text{-}O^-)Cl]^{2+}$ is shown in Figure 1, including the atom-labeling scheme. Compound III is a dinuclear Cu(II) complex of the same dinucleating ligand as compounds I, II, IV, and V. The two cupric ions are bridged by an endogenous phenolate and an exogenous chloride moiety. This compound is the chloro-bridged analogue of compounds I, II, IV, and V.

The cupric atoms are both pentacoordinate with ligation to two pyridyl nitrogens, one amine nitrogen, a phenolate oxygen, and chloride. The geometry about each copper is best described as distorted tetragonal with the basal plane around Cu1 being comprised of N1, N2, O1, and Cl and the basal plane around Cu2 consisting of N4, N5, O1, and Cl. Cu1 lies 0.32 Å above its basal plane in the direction of its axial ligand, N3. Cu2 sits 0.29 Å out of its equatorial plane in the direction of its apical ligand, N6. Analysis of the shape-determining angles using the approach of Muetterties and Guggenberger[17] yields values for e_3 of 14.1° for Cu1 and 8.6° for Cu2 (Table VIII). In this method the important dihedral angles (known as the shape-determining angles, e_1, e_2, and e_3) can be calculated in order to describe a complex geometry. The two possible limiting geometries for a five-coordinate metal center are trigonal bipyramidal and square-based pyramidal. The key shape-determining angle, e_3, is 0.0° for ideal square-based-pyramidal complexes and 53.1° for ideal trigonal-bipyramidal complexes. The geometry around the copper atoms for III deviates from ideal tetragonal geometry more than that of the compounds I, II, and IV, but less than that of the compound V. The dihedral angle between the two basal planes (N1N2O1Cl and N4N5O1Cl) is 8.4°. The copper atoms are crystallographically independent with an approximate twofold axis passing through C4, C7, O1, and Cl. The $Cu_2(O)(Cl)$ unit is nearly planar with the maximum deviation of any of the four atoms from the best least-squares plane being 0.02 Å. N1 is trans to the exogenous bridging ligand (Cl), N2 is trans to O1, N4 is trans to the exogenous bridge, and N5 is trans to O1. Equatorial copper–ligand bond lengths and the axial copper–ligand distances (Cu1–N3, Cu2–N6) are given in Table II. All of these distances are in ranges expected for cupric compounds with this geometry. The copper–copper separation is 3.265 Å. This distance is longer than that observed in compounds I, II, and IV. An increase in the Cu1–O1–Cu2 angle 111.4 (3)° is observed to accompany the increased copper–copper separation (Table VIII).

$[Cu_2(L\text{-}O^-)OMe][BPh_4]_2$ (IV). Final positional parameters are given in Table VI; selected bond distances and angles are found in Table III. An ORTEP view with the atom-labeling scheme is shown in Figure 2.

(17) Muetterties, E. L.; Guggenberger, L. J. *J. Am. Chem. Soc.* **1974**, *96*, 1748–1756.

Table II. Selected Bond Distances and Angles for Compound III (X = Chloride)

	(A) Bond Distances (Å)		
Cu1–O1	1.987 (7)	Cu1–Cl	2.316 (3)
Cu1–N1	2.070 (8)	Cu1–N2	1.964 (7)
Cu1–N3	2.158 (10)	Cu2–O1	1.965 (6)
Cu2–Cl	2.316 (3)	Cu2–N4	2.068 (9)
Cu2–N5	1.972 (7)	Cu2–N6	2.152 (11)
	(B) Bond Angles (deg)		
O1–Cu1–Cl	79.2 (2)	O1–Cu1–N1	93.1 (3)
O1–Cu1–N2	164.2 (3)	O1–Cu1–N3	92.1 (4)
Cl–Cu1–N1	156.0 (3)	Cl–Cu1–N2	88.1 (2)
Cl–Cu1–N3	104.8 (3)	N1–Cu1–N2	94.7 (3)
N1–Cu1–N3	98.1 (3)	N2–Cu1–N3	100.3 (4)
O1–Cu2–Cl	79.7 (2)	O1–Cu2–N4	91.4 (3)
O1–Cu2–N5	164.1 (3)	O1–Cu2–N6	94.7 (7)
Cl–Cu2–N4	160.4 (4)	Cl–Cu2–N5	88.9 (2)
Cl–Cu2–N6	102.6 (2)	N4–Cu2–N5	92.8 (3)
N4–Cu2–N6	96.4 (4)	N5–Cu2–N6	98.6 (3)
Cu1–O1–Cu2	111.4 (3)	Cu1–Cl–Cu2	89.6 (1)
Cu1–O1–C7	125.3 (5)	Cu2–O1–C7	123.1 (5)

Table III. Selected Bond Distances and Angles for Compound IV (X = Methoxide)

	(A) Bond Distances (Å)		
Cu1–O1	2.020 (17)	Cu1–O2	1.933 (21)
Cu1–N1	2.068 (26)	Cu1–N3	2.211 (29)
Cu1–N2	1.996 (21)	Cu2–O1	1.952 (19)
Cu2–O2	1.952 (19)	Cu2–N4	2.062 (19)
Cu2–N5	1.997 (23)	Cu2–N6	2.251 (27)
	(B) Bond Angles (deg)		
O1–Cu1–O2	73.8 (8)	O1–Cu1–N1	91.1 (9)
O2–Cu1–N1	156.0 (10)	O1–Cu1–N3	95.3 (9)
O2–Cu1–N3	104.9 (10)	N1–Cu1–N3	94.9 (11)
O1–Cu1–N2	166.5 (9)	O2–Cu1–N2	95.8 (9)
N1–Cu1–N2	95.8 (9)	N3–Cu1–N2	95.8 (10)
O1–Cu2–O2	74.9 (8)	O1–Cu2–N4	90.2 (8)
O2–Cu2–N4	155.8 (9)	O1–Cu2–N5	169.5 (9)
O2–Cu2–N5	98.4 (9)	N4–Cu2–N5	93.2 (8)
O1–Cu2–N6	90.5 (9)	O2–Cu2–N6	100.3 (9)
N4–Cu2–N6	98.8 (9)	N5–Cu2–N6	98.8 (10)
Cu1–O1–Cu2	103.9 (8)	Cu1–O1–C7	126.9 (18)
Cu2–O1–C7	128.1 (17)	Cu2–O1–Cu2	107.3 (9)

Table IV. Selected Bond Distances and Angles for Compound V (X = Bromide)

	(A) Bond Distances (Å)		
Cu1–Br	2.483 (6)	Cu1–N2	1.955 (29)
Cu1–O1	1.989 (15)	Cu1–N3	2.126 (19)
Cu1–N1	2.009 (34)		
	(B) Bond Angles (deg)		
O1–Cu1–Br	80.3 (7)	N1–Cu1–N2	92.6 (14)
O1–Cu1–N1	93.5 (14)	N1–Cu1–N3	98.5 (11)
O1–Cu1–N2	166.4 (10)	N2–Cu1–N3	95.6 (10)
O1–Cu1–N3	95.5 (9)	Cu1–O1–Cu1′	114.6 (13)
Br–Cu1–N1	151.9 (9)	Cu1–Br–Cu1′	84.8 (3)
Br–Cu1–N2	88.6 (8)	Cu1–O1–C7	122.7 (6)
Br–Cu1–N3	109.4 (7)		

Compound IV is a binuclear copper complex doubly bridged by an exogenous methoxide and an endogenous phenolate donor. Each cupric ion is pentacoordinate with ligation to the two pyridyl nitrogens, one amino nitrogen, and bridging phenolate, O1, and methoxide, O2, oxygen donors. The copper atoms are crystallographically independent with an approximate twofold axis running through C4, C7, O1, and O2.

The coordination geometry about each copper ion is distorted tetragonal with the shape-determining angles of 9.5° for Cu1 and 11.4° for Cu2. N1, N2, O1, and O2 occupy the basal plane around Cu1, while the basal plane around Cu2 is made up of N4, N5, O1, and O2. The axial positions are occupied by the pyridyl nitrogens N3 and N6, respectively. Cu1 lies 0.26 Å and Cu2 lies 0.25 Å out of their respective basal planes in the directions of N3 and N6, respectively. The angle between the two basal planes

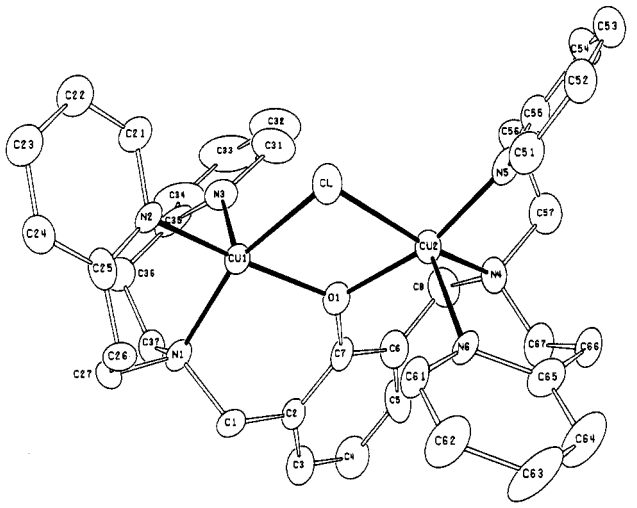

Figure 1. ORTEP diagram of the cationic portion of the chloro-bridged dinuclear complex $[Cu_2(L\text{-}O^-)Cl]^{2+}$ (III^{2+}), showing 50% probability ellipsoids and the atom-labeling scheme.

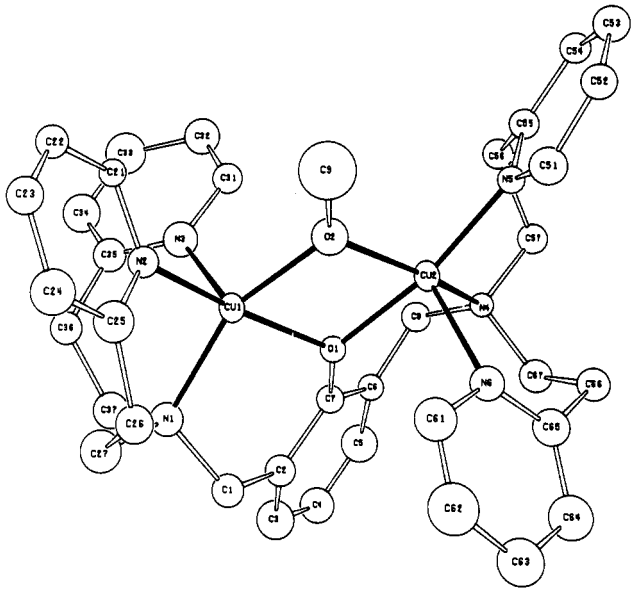

Figure 2. ORTEP diagram of the cationic portion of the methoxide-bridged dinuclear complex $[Cu_2(L\text{-}O^-)OMe]^{2+}$ (IV^{2+}), showing 50% probability ellipsoids and the atom-labeling scheme.

is 9.6°. The Cu_2O_2 ring is essentially planar, the largest deviation of any of the four atoms from the best least-squares plane being 0.016 Å. The copper–copper separation is 3.128 Å.

The copper–ligand bond distances are in the range observed for analogous five-coordinate cupric complexes with tetragonal coordination geometries (Table VIII).[18-20] Equatorial copper–ligand bond lengths and the axial copper–ligand distances (Cu1–N3, Cu2–N6) are given in Table III.

$[Cu_2(L\text{-}O^-)Br][PF_6]_2\cdot 0.5CH_2Cl_2$ (V). Final positional parameters are given in Table VII; selected bond distances and angles are found in Table IV. An ORTEP view with the atom-labeling scheme is shown in Figure 3.

This compound is the dinuclear bromo-bridged analogue of compounds I–IV. A crystallographic twofold axis passes through

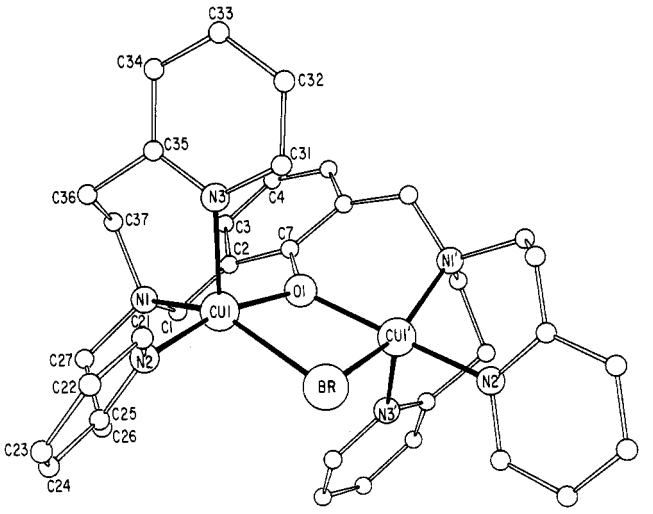

Figure 3. ORTEP diagram of the cationic portion of the bromo-bridged dinuclear complex $[Cu_2(L\text{-}O^-)Br]^{2+}$ (V^{2+}), showing 50% probability ellipsoids and the atom-labeling scheme.

C4, C7, Br, and O1; thus the coordination geometries around the two copper centers are identical. Each cupric ion is pentacoordinate with ligation to the N_3 tridentate donor unit, the phenolate oxygen, and bromide donors. The copper centers are doubly bridged by O1 and Br. The coordination geometry around each copper atom is distorted square-based pyramidal. The basal plane is formed by O1, N1, N2, and Br, and the axial position is occupied by N3. The angle between the two planes O1N1N2Br and O1N1′N2′Br is 4.9°. Muetterties–Guggenberger analysis gives a shape-determining angle of 21.0°.[5] The coordination geometry thus deviates from ideal tetragonal geometry more than in compounds I–IV (Table VIII). The $Cu_2(Br)(O)$ unit is rigorously planar as shown by the crystallographic twofold axis. The bond distances observed for this compound are in the range seen for previously discussed and published compounds (Table VIII).[18,22] The equatorial copper–ligand bond distances are Cu–Br = 2.483 (6) Å, Cu–O1 = 1.989 (15) Å, Cu1–N1 = 2.009 (34) Å, and Cu–N2 = 1.955 (29) Å, and the axial bond length is Cu–N3 = 2.126 (19) Å. The copper–copper separation is, as expected, the largest of the series I–IV, and the Cu–O–Cu angle is 114.6 (13)°.

Comparison of Compounds I–V. Table VIII contains selected structural parameters for the five compounds I–V. These compounds are all structurally very similar. Each possesses cupric ions that have distorted square-based-pyramidal geometries. The shape-determining angles range from the near-ideal tetragonal value of 1.2° for compound I to the most distorted value of 21.0° for compound V. The basal planes, in all five cases, are made up of an amine nitrogen (N1 and N4), a pyridyl nitrogen (N2 and N5), a phenolate oxygen (O1), and X, where X = azide, hydroxide, chloride, methoxide, or bromide. A pyridyl nitrogen (N3 and N6) serves as an axial ligand in all five compounds. The copper–amine distances are all in the 2.009 (39)–2.070 (8) Å range, and equatorial copper–pyridine distances are found to be in the 1.955 (29)–2.006 (16) Å range.

Except for Cu–O1 in compound IV nd Cu1–O1 in compound II, all of the copper–phenolate distances are in the 1.952 (19)–1.989 (15) Å range. The Cu–O1 distance in compound IV is slightly longer, 2.070 (17) Å, whereas the Cu–O1 distance in compound II is shorter, 1.933 (14) Å. The axial copper–pyridine distances range from 2.126 (19) to 2.258 (13) Å. However, a consistent observation for these compounds is that the equatorial copper–pyridine distances are at least 0.1 Å shorter than the axial

(18) (a) Sorrell, T. N.; Malachowski, M. R.; Jameson, D. L. *Inorg. Chem.* **1982**, *21*, 3250–3252. (b) Martin, A. E.; Lippard, S. J. *J. Am. Chem. Soc.* **1984**, *106*, 2579–2583.
(19) Coughlin, P. K.; Lippard, S. J. *J. Am. Chem. Soc.* **1981**, *103*, 3228–3229.
(20) Agnus, Y.; Louis, R.; Gisselbrecht, J. P.; Weiss, R. *J. Am. Chem. Soc.* **1984**, *106*, 93–102.
(21) Marsh, W. E.; Hatfield, W. E.; Hodgson, D. J. *Inorg. Chem.* **1982**, *21*, 2679–2684.
(22) (a) Singh, P.; Copeland, V. C.; Hatfield, W. E.; Hodgson, D. J. *J. Phys. Chem.* **1972**, *76*, 2887–2891. (b) Alnscough, E. W.; Baker, E. N.; Brodie, A. M.; Larsen, N. G. *J. Chem. Soc., Dalton Trans.* **1981**, 2054–2058. (c) Birker, P. J.; Godefroi, E. F.; Helder, J.; Reedijk, J. *J. Am. Chem. Soc.* **1982**, *104*, 7556–7560.

Table V. Atom Coordinates ($\times 10^4$) and Temperature Factors ($\times 10^3$ Å^2) for Compound II

atom	x	y	z	$U_{equiv/iso}$	atom	x	y	z	$U_{equiv/iso}$
Cu1	3586 (1)	2204 (1)	2507 (1)	40 (1)*	C37	5222 (11)	3317 (7)	3476 (5)	53 (5)*
Cu2	3104 (1)	37 (1)	2398 (1)	43 (1)*	C67	4513 (13)	−1319 (7)	3000 (5)	64 (6)*
O(1)	4072 (7)	1071 (4)	2843 (3)	45 (3)*	C5	5844 (9)	259 (5)	4166 (3)	78 (7)*
Cl	2312 (3)	1180 (2)	1859 (1)	65 (1)*	C4	6924 (9)	853 (5)	4237 (3)	83 (7)*
N1	5244 (8)	2920 (5)	2893 (4)	40 (4)*	C3	7050 (9)	1520 (5)	3840 (3)	70 (6)*
C64	5693 (9)	−1414 (4)	1609 (4)	103 (8)*	C2	6095 (9)	1593 (5)	3371 (3)	45 (5)*
C63	6152 (9)	−818 (4)	1228 (4)	116 (9)*	C7	5015 (9)	999 (5)	3299 (3)	45 (5)*
C62	5828 (9)	49 (4)	1213 (4)	87 (7)*	C6	4890 (9)	332 (5)	3697 (3)	55 (5)*
C61	5045 (9)	319 (4)	1579 (4)	58 (5)*	C24	3507 (8)	4146 (5)	1222 (3)	52 (5)*
N6	4586 (9)	−278 (4)	1960 (4)	48 (4)*	C23	2252 (8)	4270 (5)	1095 (3)	59 (6)*
C65	4910 (9)	−1144 (4)	1975 (4)	61 (6)*	C22	1413 (8)	3828 (5)	1408 (3)	57 (5)*
N4	3444 (10)	−827 (5)	3069 (4)	48 (4)*	C21	1828 (8)	3262 (5)	1846 (3)	54 (5)*
C34	2596 (10)	3058 (7)	4154 (3)	105 (9)*	N2	3083 (8)	3138 (5)	1973 (3)	42 (4)*
C33	1648 (10)	2411 (7)	4240 (3)	121 (10)*	C25	3923 (8)	3580 (5)	1661 (3)	48 (5)*
C32	1138 (10)	1776 (7)	3798 (3)	101 (8)*	C66	4430 (12)	−1734 (7)	2401 (5)	59 (5)*
C31	1576 (10)	1787 (7)	3270 (3)	84 (7)*	C8	3734 (12)	−302 (7)	3642 (5)	64 (5)*
N3	2523 (10)	2434 (7)	3183 (3)	57 (4)*	C36	4046 (10)	3723 (7)	3511 (5)	62 (5)*
C35	3033 (10)	3069 (7)	3625 (3)	63 (6)*	C26	5204 (10)	3424 (7)	1856 (5)	51 (5)*
C57	2321 (12)	−1484 (8)	3107 (5)	66 (6)*	C56	1119 (11)	−1134 (8)	2880 (5)	63 (5)*
C27	5597 (10)	3662 (7)	2508 (5)	47 (5)*	C1	6254 (10)	2315 (7)	2948 (5)	49 (5)*
C51	1634 (7)	−890 (5)	1351 (3)	55 (5)*	B1	7285 (13)	6567 (8)	3864 (5)	41 (5)*
C52	598 (7)	−1394 (5)	1028 (3)	58 (6)*	B2	−2854 (13)	2787 (8)	213 (6)	47 (6)*
C53	−319 (7)	−1806 (5)	1311 (3)	71 (6)*	C132	8029 (6)	5294 (4)	4571 (3)	50 (3)
C54	−199 (7)	−1713 (5)	1916 (3)	62 (6)*	C133	8554 (6)	4504 (4)	4690 (3)	57 (3)
C134	8894 (6)	4012 (4)	4241 (3)	53 (3)	C126	7355 (6)	6744 (4)	2746 (3)	48 (3)
C135	8708 (6)	4311 (4)	3673 (3)	57 (3)	C121	6601 (6)	6529 (4)	3159 (3)	43 (3)
C136	8182 (6)	5101 (4)	3554 (3)	48 (3)	C102	5410 (7)	5980 (4)	4408 (3)	53 (3)
C131	7842 (6)	5592 (4)	4004 (3)	39 (3)	C103	4455 (7)	6087 (4)	4720 (3)	65 (4)
C143	7670 (7)	4241 (5)	868 (3)	56 (3)	C104	4259 (7)	6936 (4)	4903 (3)	70 (4)
C144	8042 (7)	4744 (5)	1389 (3)	60 (4)	C105	5018 (7)	7678 (4)	4775 (3)	67 (4)
C145	8403 (7)	4324 (5)	1909 (3)	66 (4)	C106	5972 (7)	7571 (4)	4463 (3)	58 (3)
C146	8391 (7)	3402 (5)	1907 (3)	59 (4)	C101	6168 (7)	6722 (4)	4280 (3)	43 (3)
C142	8019 (7)	2899 (5)	1386 (3)	54 (3)	C112	8233 (6)	8249 (5)	3829 (3)	59 (4)
C141	7658 (7)	3318 (5)	867 (3)	46 (3)	C113	9143 (6)	8964 (5)	3998 (3)	72 (4)
C152	9079 (7)	3671 (4)	−153 (2)	44 (3)	C114	10245 (6)	8834 (5)	4365 (3)	70 (4)
C153	9735 (7)	3964 (4)	−589 (2)	57 (3)	C115	10439 (6)	7988 (5)	4564 (3)	73 (4)
C154	9202 (7)	3806 (4)	−1175 (2)	54 (3)	C116	9529 (6)	7272 (5)	4394 (3)	53 (3)
C155	8012 (7)	3354 (4)	−1325 (2)	56 (3)	C111	8427 (6)	7403 (5)	4027 (3)	40 (3)
C156	7356 (7)	3060 (4)	−889 (2)	52 (3)	C171	−2456 (7)	1719 (4)	232 (3)	45 (3)
C151	7889 (7)	3218 (4)	−304 (2)	43 (3)	C172	−1272 (7)	1547 (4)	496 (3)	57 (3)
C162	4901 (7)	2249 (4)	407 (3)	59 (4)	C173	−927 (7)	689 (4)	467 (3)	70 (4)
C163	3623 (7)	2290 (4)	337 (3)	69 (4)	C174	−1765 (7)	2 (4)	175 (3)	66 (4)
C164	3072 (7)	2900 (4)	−36 (3)	85 (5)	C175	−2948 (7)	174 (4)	−89 (3)	58 (4)
C165	3798 (7)	3469 (4)	−338 (3)	81 (4)	C176	−3294 (7)	1032 (4)	−60 (3)	47 (3)
C166	5075 (7)	3428 (4)	−268 (3)	71 (4)	Sol1	796 (13)	6496 (9)	2725 (6)	165 (5)
C161	5627 (7)	2818 (4)	104 (3)	45 (3)	Sol2	1395 (17)	5934 (12)	3040 (8)	130 (6)
C122	5382 (6)	6142 (4)	2980 (3)	48 (3)	Sol3	1530 (15)	5083 (11)	2788 (7)	110 (6)
C123	4918 (6)	5970 (4)	2388 (3)	56 (3)	Sol4	1556 (18)	6120 (13)	3676 (9)	148 (7)
C124	5673 (6)	6185 (4)	1975 (3)	55 (3)	Sol5	7696 (24)	−79 (16)	2681 (11)	120 (8)
C125	6891 (6)	6572 (4)	2154 (3)	59 (4)	Sol6	8709 (24)	1392 (18)	2717 (11)	128 (9)
C55	838 (7)	−1209 (5)	2238 (3)	53 (5)*	Sol7	9023 (22)	699 (15)	1952 (11)	107 (8)
N5	1754 (7)	−797 (5)	1956 (3)	47 (4)*	Sol8	8672 (29)	567 (22)	2563 (14)	108 (10)

[a] An asterisk denotes an equivalent isotropic U value, defined as one-third of the trace of the orthogonalized U_{11} tensor.

copper–pyridine bond lengths. The mean axial copper–pyridine distance for these compounds is 2.19 Å, whereas the mean equatorial copper–pyridine distance is 1.98 Å. The copper–copper separations range from 3.082 Å in compound I to 3.348 Å in compound V. The Cu–O1–Cu angle ranges from 103.9 (8)°, in compound IV, to 114.6 (13)°, in compound V. The four-membered $Cu_2(O)(X)$ unit is strictly planar in compound V, but it is slightly distorted in compounds I–IV, with the dihedral angle between the O1Cu1X and O1Cu2X planes being 1.8, 2.3, 1.8, and 2.3° for compounds I–IV, respectively.

Magnetic Properties. None of the dicopper(II) complexes I–VII exhibit an EPR spectrum (DMF–$CHCl_3$ (1:1), 77 K), which is consistent with the occurrence of antiferromagnetic coupling between ligand-bridged Cu(II) ions in these complexes. This conclusion is borne out by magnetochemical measurements, including variable-temperature magnetic susceptibility studies carried out on compounds I–III and V. The singlet–triplet splitting, $2J$ (J is negative for an antiferromagnetic interaction), varies systematically with the coordination geometry about the $Cu_2(O)(X)$ core, with the hydroxo-bridged complex I exhibiting the greatest degree of antiferromagnetic coupling ($-2J = 600$ cm^{-1}, Table VIII). The coupling is weaker for the azido-bridged complex II and somewhat weaker for the halide-bridged compounds III and V ($-2J = 335$ cm^{-1}). The $-2J$ value for VII (X = $CH_3CO_2^-$) can be estimated to be ca. 200 cm^{-1} on the basis of a room-temperature magnetic moment of 1.56 μ_B/Cu, from recently tabulated data.[38]

The related structural trends here are that the most strongly coupled complex I possesses the shortest Cu···Cu distance or, more importantly, (a) the smallest $Cu–O_{phenolate}–Cu$ bridging angle and (b) the largest Cu–X–Cu bridging angle (Table VIII). From extensive studies by Hatfield and co-workers[40] on $[(\mu\text{-X})Cu^{II}]_2$ dimers (X = OH^-, halide, etc.) it is likely that the Cu–X–Cu angle is the most important determinant in the sign and magnitude of the magnetic coupling between Cu(II) ions. According to these studies, and on the basis of the bridging through the phenolate oxygen atom, the extent of antiferromagnetic coupling should increase in the order $OH^- < \mu\text{-}1,1\text{-}N_3^- < Cl^- < Br^-$, as the $Cu–O_{phenolate}–Cu$ angle increases on going from complex I to the X-bridged complexes II, III, and V. (Note: The $Cu–O_{phenolate}$

Table VI. Atom Coordinates ($\times 10^4$) and Temperature Factors ($\times 10^3$ Å^2) for Compound IV

atom	x	y	z	$U_{equiv/iso}$[a]	atom	x	y	z	$U_{equiv/iso}$[a]
Cu1	3074 (4)	67 (3)	2431 (2)	37 (2)*	C101	8378 (15)	7388 (16)	3973 (8)	28 (10)
Cu2	3571 (4)	2156 (3)	2532 (2)	36 (2)*	C102	8086 (15)	8223 (17)	3767 (8)	47 (11)
O1	4098 (15)	1087 (12)	2934 (8)	29 (6)	C103	8962 (15)	8977 (16)	3912 (8)	46 (11)
O2	2557 (18)	1154 (14)	2071 (9)	52 (7)	C104	10129 (15)	8896 (16)	4264 (8)	64 (13)
N1	3435 (23)	-813 (18)	3106 (11)	46 (9)	C105	10421 (15)	8061 (16)	4470 (8)	65 (13)
N2	1735 (19)	-758 (16)	1928 (10)	35 (8)	C106	9546 (15)	7307 (16)	4324 (8)	53 (12)
N3	4636 (23)	-262 (21)	2000 (12)	55 (9)	C111	7884 (19)	5610 (16)	4006 (8)	31 (10)
N4	5214 (19)	2889 (15)	2946 (10)	25 (8)	C112	8272 (19)	5120 (16)	3571 (8)	78 (14)
N5	3096 (19)	3137 (15)	1989 (10)	29 (8)	C113	8807 (19)	4328 (16)	3709 (8)	66 (13)
N6	2341 (22)	2379 (17)	3194 (11)	44 (9)	C114	8953 (19)	4025 (16)	4282 (8)	50 (11)
C1	3706 (25)	-324 (20)	3694 (14)	44 (11)	C115	8564 (19)	4515 (16)	4717 (8)	55 (12)
C2	4862 (28)	322 (21)	3770 (15)	42 (11)	C116	8030 (19)	5307 (16)	4580 (8)	69 (13)
C3	5817 (32)	207 (24)	4229 (16)	69 (13)	C121	6171 (21)	6698 (12)	4255 (9)	31 (10)
C4	6865 (32)	771 (22)	4322 (15)	60 (12)	C122	5369 (21)	5956 (12)	4370 (9)	62 (13)
C5	6977 (30)	1410 (23)	3941 (14)	68 (13)	C123	4380 (21)	6067 (12)	4672 (9)	52 (12)
C6	6079 (24)	1588 (20)	3448 (13)	31 (10)	C124	4213 (21)	6920 (12)	4860 (9)	67 (13)
C7	5066 (26)	1029 (20)	3367 (13)	34 (10)	C125	5015 (21)	7662 (12)	4746 (9)	72 (13)
C8	6218 (25)	2267 (19)	3021 (13)	41 (11)	C126	5994 (21)	7551 (12)	4443 (9)	47 (11)
C9	1495 (36)	1163 (29)	1597 (18)	157 (21)	C131	6564 (14)	6467 (12)	3130 (10)	30 (11)
C21	1618 (24)	-881 (18)	1329 (12)	28 (10)	C132	7311 (14)	6691 (12)	2709 (10)	43 (11)
C22	558 (26)	-1390 (19)	1029 (14)	37 (11)	C133	6810 (14)	6538 (12)	2114 (10)	58 (12)
C23	-360 (30)	-1716 (20)	1279 (14)	44 (11)	C134	5562 (14)	6161 (12)	1940 (10)	57 (10)
C24	-291 (29)	-1645 (22)	1869 (14)	65 (13)	C135	4815 (14)	5937 (12)	2361 (10)	64 (13)
C25	792 (29)	-1159 (22)	2192 (16)	57 (12)	C136	5316 (14)	6090 (12)	2956 (10)	51 (12)
C26	1009 (25)	-1156 (21)	2854 (14)	50 (12)	C201	7693 (17)	3291 (16)	883 (9)	35 (11)
C27	2272 (27)	-1540 (22)	3105 (15)	66 (13)	C202	7734 (17)	4149 (16)	917 (98)	58 (12)
C31	5122 (25)	402 (22)	1169 (13)	41 (11)	C203	8142 (17)	4602 (16)	1457 (9)	56 (12)
C32	6040 (28)	262 (24)	1364 (15)	62 (12)	C204	8509 (17)	4126 (16)	1961 (9)	49 (12)
C33	6481 (32)	-629 (25)	1381 (16)	84 (14)	C205	8468 (17)	3197 (16)	1927 (9)	57 (12)
C34	5947 (28)	-1272 (24)	1729 (14)	70 (13)	C206	8060 (17)	2743 (16)	1387 (9)	39 (11)
C35	5055 (29)	-1055 (25)	2027 (14)	51 (12)	C211	7898 (19)	3201 (13)	-261 (7)	17 (9)
C36	4494 (27)	-1679 (20)	2436 (14)	46 (11)	C212	9104 (19)	3666 (13)	-121 (7)	42 (11)
C37	4490 (28)	-1378 (22)	3069 (14)	57 (12)	C213	9752 (19)	3953 (13)	-567 (7)	49 (11)
C51	1879 (27)	3317 (21)	1881 (14)	50 (4)	C214	9194 (19)	3775 (13)	-1153 (7)	40 (11)
C52	1477 (27)	3879 (19)	1413 (13)	43 (11)	C215	7989 (19)	3310 (13)	-1293 (7)	31 (10)
C53	2350 (25)	4292 (20)	1100 (14)	48 (11)	C216	7341 (19)	3024 (13)	-847 (7)	42 (11)
C54	3572 (26)	4137 (20)	1240 (13)	37 (11)	C221	7449 (14)	1679 (14)	224 (8)	15 (9)
C55	3902 (26)	3518 (21)	1682 (14)	36 (11)	C222	6548 (14)	1024 (14)	-77 (8)	38 (11)
C56	5245 (25)	3402 (21)	1914 (13)	41 (11)	C223	6840 (14)	148 (14)	-125 (8)	38 (11)
C57	5564 (26)	3639 (19)	2583 (13)	40 (11)	C224	8031 (14)	-72 (14)	129 (8)	25 (10)
C61	1425 (30)	1699 (24)	3249 (16)	63 (13)	C225	8932 (14)	583 (14)	430 (8)	49 (12)
C62	1009 (33)	1647 (25)	3759 (17)	87 (15)	C226	8640 (14)	1459 (14)	478 (8)	36 (11)
C63	1486 (28)	2232 (22)	4231 (16)	75 (13)	C231	5621 (20)	2854 (13)	126 (9)	36 (11)
C64	2397 (29)	2931 (23)	4157 (15)	71 (13)	C232	5154 (20)	3518 (13)	-242 (9)	61 (12)
C65	2830 (28)	2989 (21)	3615 (14)	51 (11)	C233	3870 (20)	3622 (13)	-335 (9)	76 (14)
C66	3863 (24)	3675 (19)	3513 (13)	43 (11)	C234	3052 (20)	3061 (13)	-61 (9)	45 (11)
C67	5115 (26)	3299 (21)	3511 (13)	47 (11)	C235	3519 (20)	2396 (13)	307 (9)	47 (11)
B1	7274 (32)	6602 (25)	3852 (16)	31 (13)	C236	4803 (20)	2293 (13)	400 (9)	38 (11)
B2	7204 (32)	2725 (25)	233 (17)	31 (13)					

[a] An asterisk denotes an equivalent isotropic U value, defined as one-third of the trace of the orthogonalized U_{ij} tensor.

distance is essentially constant.) However, the opposite trend is observed with $-2J$ varying according to Cl^-, $Br^- < \mu$-1,1-N_3^- < OH^-. The Cu–X–Cu angle decreases in the series X = N_3^-, Cl^-, and Br^- because both the X atom and the M–X distance become larger. Thus, the exogenous bridge X must be considered to cause a reduction in the expected antiferromagnetic coupling on going from I to V (excluding IV) and the effect is greatest for the Br^- complex V, which possesses the smallest Cu–X–Cu angle. In summary, the two possible superexchange pathways are in opposition to one another. Overall, the Cu–O–Cu pathway dominates and gives rise to reasonably strong antiferromagnetic coupling. The Cu–X–Cu pathway modulates the extent of coupling and is overwhelmed by the Cu–O–Cu effect.

It is also of interest to compare the magnetic properties of I and II with those of complexes studied by Sorrell and co-workers,[26] in which pyrazole donors are used instead of pyridine groups in otherwise essentially identical ligand–dicopper(II) complexes. Complex I exhibits much stronger coupling than Sorrell's corresponding hydroxo- and phenolate-bridged compound ($-2J$ = 420 vs. 600 cm^{-1} for I, in spite of the fact that both the Cu–$O_{phenolate}$–Cu and the Cu–$O_{hydroxo}$–Cu angles are extremely close (101.9 vs. 102.5° for I and 103.6 vs. 102.5° for I, respectively). This may be due to coordination geometry differences, since Sorrell's OH^--bridged complex contains one square-pyramidal plus one trigonal-bipyramidal Cu(II) ion in the dinuclear unit, a situation that is likely to give rise to less efficient superexchange overlap and therefore weaker magnetic coupling.[26]

Sorrell's μ-1,1-N_3^--bridged complex, which is analogous to II, has a singlet–triplet separation ($-2J$ = 450 cm^{-1}) which is similar to that of his hydroxo-bridged species and close to the $-2J$ value of 440 cm^{-1} observed in II. Kahn has stated that a μ-1,1-azide bridge may lead to a ferromagnetic interaction, and he has reported that a μ-1,1-azido–μ-hydroxo Cu(II) dimer is ferromagnetic even though the hydroxo bridge is in a position to promote antiferromagnetic coupling.[39] The difference in $-2J$ between Sorrell's OH^- and μ-1,1-N_3^- complexes indicates that μ-1,1-N_3^- does not need to lead to ferromagnetism or lessen the extent of antiferromagnetic coupling.[26]

However, in our systems the dramatic decrease in $-2J$ as we go from I to II does lend experimental support to the prediction of a ferromagnetic coupling through a 1,1-azido bridge, since the Cu–$O_{phenolate}$–Cu angle increases from 102.5 to 107.9° (which should increase $-2J$), while the Cu–X–Cu angle decreases insignificantly (from 104.4 to 103.6°). It should be noted that μ-1,3-N_3^--bridged complexes always exhibit extremely strong antiferromagnetic coupling,[25,26a,b] allowing magnetism to be useful

Table VII. Atom Coordinates ($\times 10^4$) and Temperature Factors ($\times 10^3$ Å^2) for Compound V

atom	x	y	z	$U_{equiv/iso}$[a]
Cu1	596 (3)	1263 (1)	1825 (4)	54 (3)*
Br	0	700 (1)	2500	66 (5)*
O1	0	1593 (8)	2500	81 (30)*
N1	1727 (25)	1701 (8)	2315 (30)	99 (9)
C1	2017 (26)	1972 (9)	3418 (32)	78 (10)
C2	1036 (28)	2189 (11)	2989 (34)	82 (10)
C3	969 (40)	2629 (14)	2956 (47)	161 (18)
C4	0	2828 (18)	2500	122 (20)
C7	0	2029 (16)	2500	93 (16)
C21	598 (15)	579 (7)	381 (20)	91 (11)
C22	1107 (15)	249 (7)	289 (20)	148 (16)
C23	2328 (15)	191 (7)	1343 (20)	166 (18)
C24	3040 (15)	463 (7)	2488 (20)	154 (17)
C25	2531 (15)	793 (7)	2580 (20)	115 (13)
N2	1311 (15)	851 (7)	1526 (20)	111 (8)
C26	3168 (30)	1086 (9)	3592 (34)	98 (12)
C27	2930 (34)	1507 (11)	2996 (42)	127 (14)
C31	−1973 (19)	1285 (5)	−1056 (22)	79 (10)
C32	−2938 (19)	1417 (5)	−2443 (22)	105 (12)
C33	−2763 (19)	1670 (5)	−3147 (22)	106 (13)
C34	−1622 (19)	1790 (5)	−2462 (22)	106 (12)
C35	−657 (19)	1658 (5)	−1075 (22)	90 (11)
N3	−832 (19)	1405 (5)	−372 (22)	109 (8)
C36	639 (27)	1725 (10)	−251 (35)	95 (11)
C37	1196 (31)	1995 (10)	1042 (36)	106 (13)
P1	5000	2083 (6)	2500	91 (15)*
P2	5000	559 (5)	7500	104 (20)*
F11	6229 (29)	1898 (10)	3587 (34)	129 (11)
F12	4907 (19)	2115 (7)	3632 (24)	102 (8)
F13	5000	2550 (21)	2500	307 (29)
F14	6226 (40)	2314 (14)	3664 (47)	134 (16)
F15	4983 (41)	1669 (14)	3147 (48)	139 (17)
F21	5000	80 (11)	7500	150 (12)
F22	5000	1035 (11)	7500	155 (13)
F23	3636 (22)	560 (7)	6101 (26)	146 (9)
F24	5260 (19)	565 (7)	6500 (24)	147 (9)
Csol	6773 (54)	543 (19)	5606 (69)	92 (24)
Hsoa	6544	588	6114	96
Hsob	6492	280	5148	96
Cl1	6249 (21)	867 (7)	4415 (26)	140 (9)
Cl2	8331 (26)	537 (9)	6770 (32)	188 (12)

[a] An asterisk denotes an equivalent isotropic U value, defined as one-third of the trace of the orthogonalized U_{11} tensor.

as a quantitative differentiator between the two azide bridging modes.

Spectroscopy. Table IX contains the UV–vis spectral data for compounds I–VII. To summarize, we assign a strong band occurring in all the complexes in the 370–475-nm region to a PhO^- → Cu(II) LMCT transition. The position of the band depends on the bridging group, X, but the range observed is consistent with that found for other compounds described in the literature.[1,23-28] Complexes I, IV, VI, and VII also possess an absorption at 335–340 nm, assigned to a OR^--to-Cu(II) (R = H, Me, C(O)Me, C(O)Ph LMCT transition. Absorptions due to X = Cl^-, Br^- coordination are either very weak or absent. Typical broad d–d absorptions are observed in the 625–680-nm region.

By comparison to the phenolate- and OH^--bridged complex I, it is striking that both the phenolate- and halide-bridged compounds III and V do not possess an absorption in the 368–378-nm region, and they have only one charge-transfer band in the 300–500-nm region. We have previously assigned[11] the 378-nm band in compound I to a phenolate-to-Cu(II) LMCT absorption, and this has been confirmed in a resonance Raman study.[36] It is known that chloride-to-copper LMCT absorptions are relatively weak[1,29] and they are completely absent in Cl^--containing Cu(II) complexes of the PY2 (PY2 = bis(2-(2-pyridyl)ethyl)amine) tridentate moiety.[13] Thus, we are forced to assign the 451-nm band in III and the 475-nm absorption in V to phenolate → Cu(II) LMCT transitions.

The position of the phenolate-to-copper charge-transfer transition is sensitive to the ligand environment, the presence of chelating ligands, and the electron density on the copper atom.[30] Furthermore, Suzuki has reported that the shift of the phenolate-to-copper LMCT band is related to the Cu–O–Cu bridging angle.[23] This seems to be the case here, where there is a general shifting to lower energy of the LMCT transition for larger X. This shift of the phenolate-to-copper LMCT band in compound V thus may be related to the Cu–O1–Cu bridging angle (Table VIII) in V, the largest observed in any of the compounds I–V. Also, complex V (X = Br) possesses a copper coordination geometry most distorted from ideal tetragonal geometry, compared to those geometries of any of the other structurally characterized cupric compounds I–IV.

Compounds I, IV, VI, and VII, which contain X = oxygen atom donor, possess very similar spectral characteristics, and this reflects the close structural relationship among these particular compounds. All of these complexes exhibit phenolate-to-copper LMCT transitions at wavelengths in the 370–380-nm range and much weaker d–d transitions at lower energy (Table IX). The band at 340 nm (ϵ = 2375 M^{-1} cm^{-1}) in compound I is assigned to a ligand-to-metal charge-transfer band (LMCT), which we attribute to the hydroxide-to-copper transition. The band at 335 nm (ϵ = 2270 M^{-1} cm^{-1}) in compound IV is similarly assigned to the methoxide-to-copper LMCT transition. These assignments are consistent with those made for related cupric compounds with similar coordination geometries.[19,31] Compounds VI and VII both also

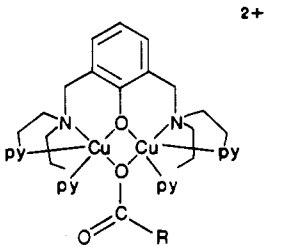

R = C_6H_5 (VI^{2+}), CH_3 (VII^{2+})

py = 2-pyridyl

exhibit a $RCOO^-$ → Cu(II) (R = C_6H_5 (VI), CH_3 (VII)) LMCT band at 335 nm. This assignment is suggested by considering the possibility that acetate and benzoate are involved in monoatomic unidentate bridging in solution. This would be consistent with the observed thermodynamic stability of the monoatomic bridged compound of I and the tendency for μ-1,1-azide and not μ-1,3-azide bridging to occur in complexes of L-O^- such as II[14] and a related analogue.[26b] The occurrence of M–O–M bridges via one of the oxygen atoms of the acetate ligand has been firmly es-

(23) Suzuki, M.; Kanatomi, H.; DeMura, Y.; Murase, I. *Bull. Chem. Soc. Jpn.* **1984**, *57*, 1003–1007.
(24) Agnus, Y.; Louis, R.; Gisselbrecht, J. P.; Weiss, R. *J. Am. Chem. Soc.* **1984**, *106*, 93–102.
(25) McKee, V.; Zvagulis, M.; Dagdigian, J. V.; Patch, M. G.; Reed, C. A. *J. Am. Chem. Soc.* **1984**, *106*, 4765–4772.
(26) (a) Sorrell, T. N.; O'Connor, C. J.; Anderson, D. P.; Reibenspies, J. H. *J. Am. Chem. Soc.* **1985**, *107*, 4199–4206. (b) Sorrell, T. N. In *Biological and Inorganic Copper Chemistry*; Karlin, K. D., Zubieta, J., Eds.; Adenine: Guilderland, NY, 1986; Vol. 2, pp 41–55, and references therein. (c) Sorrell, T. N.; Jameson, D. L.; O'Connor, C. J. *Inorg. Chem.* **1984**, *23*, 190.
(27) Himmelwright, R. S.; Eickman, N. C.; LuBien, C. D.; Solomon, E. I. *J. Am. Chem. Soc.* **1980**, *102*, 5378.
(28) Yamauchi, O.; Tsujide, K.; Odani, A. *J. Am. Chem. Soc.* **1985**, *107*, 659–666.
(29) For $[Cu(tmed)Cl_2]_2$ (tmed = tetramethylethylenediamine), the chloride-to-copper LMCT transition is at 445 nm (ϵ = 435 M^{-1} cm^{-1}): Meinders, H. C.; Van Bolhius, F.; Chella, G. *J. Mol. Catal.* **1979**, *5*, 225–233.
(30) Ainscough, E. W.; Bingham, A. G.; Brodie, A. M.; Husbands, J. M.; Plowman, J. E. *J. Chem. Soc., Dalton Trans.* **1981**, 1701–1707.
(31) (a) Kida, S.; Nishida, Y.; Sakamoto, M. *Bull. Chem. Soc. Jpn.* **1973**, *46*, 2428–2430. (b) Arcus, C.; Fivizzani, K. P.; Pavkovic, S. F. *J. Inorg. Nucl. Chem.* **1977**, *39*, 285–287. (c) Ishimura, Y.; Nonaka, Y.; Nishida, Y.; Kida, S. *Bull. Chem. Soc. Jpn.* **1973**, *46*, 3728–3733.

Table VIII. Structural and Magnetic Comparison of Compounds I–V

	I,[11] X = OH^-	II,[14] X = N_3^-	III, X = Cl^-	IV, X = OCH_3^-	V, X = Br^-
Cu1–N1, Å	2.034 (14)	2.057 (10)	2.070 (8)	2.068 (26)	2.034 (14)
Cu—N2, Å	2.006 (16)	1.985 (10)	1.964 (7)	1.996 (21)	1.955 (29)
Cu1–N3, Å	2.258 (13)	2.204 (10)	2.158 (10)	2.211 (29)	2.126 (19)
Cu1–O1, Å	1.979 (10)	1.963 (8)	1.987 (7)	2.020 (17)	1.989 (15)
Cu1–X, Å (X)	1.938 (10) (O)	2.024 (12) (N_3)	2.316 (3) (Cl)	1.933 (21) (O)	2.483 (6) (Br)
Cu2–N4, Å	2.028 (13)	2.048 (9)	2.068 (9)	2.062 (19)	...
Cu2–N5, Å	2.027 (14)	2.001 (10)	1.972 (7)	1.997 (23)	...
Cu2–N6, Å	2.149 (15)	2.141 (10)	2.152 (11)	2.251 (27)	...
Cu2–O1, Å	1.972 (11)	1.976 (8)	1.965 (6)	1.965 (6)	...
Cu2–X, Å (X)	1.962 (10) (O)	2.028 (12) (N_3)	2.316 (3) (Cl)	1.952 (19) (O)	...
Cu1–plane, Å	0.3121	0.3479	0.3221	0.2627	0.3531
Cu2–plane, Å	0.2613	0.3182	0.2908	0.2546	...
e_3(Cu1), deg	3.2	6.8	14.1	9.5	21.0
e_3(Cu2), deg	1.2	9.8	8.6	11.4	...
O1Cu1X/O1Cu2X, deg	1.8	2.3	1.8	2.3	...
N1N2O1O2/N4N5O1O2,[a] deg	4.2				
N1N2N7O1/N4N5N7O1, deg		8.1			
N1N2O1C1/N4N5O1C1, deg			8.4		
N1N2O1O2/N4N5O1O2, deg				9.6	
O1N1N2Br/O1N1′N2′Br, deg					4.9
Cu1–Cu2, Å	3.082	3.185	3.265	3.128	3.348
Cu1–O1–Cu2, deg	102.5 (5)	107.9 (3)	111.4 (3)	103.9 (8)	114.6 (13)
Cu1–X–Cu2, deg	104.4	103.6	89.6	...	84.8
−2J, cm^{-1}	600	440	335	...	335

[a] Angle between best least-squares planes defined by the atoms listed.

Table IX. Selected UV–Vis Absorptions (CH_3CN) for Compounds I–VII[a]

I,[11] X = OH^-	II,[14] X = N_3^-	III, X = Cl^-	IV, X = OMe^-	V, X = Br^-	VI, X = OBz^-	VII, X = OAc^-	assignt
			Solution Spectra				
			Ligand to Cu LMCT				
340 (2375)	...	...	...	...	...	...	$OH^- \rightarrow Cu$
...	...	...	335 (2270)	...	...	...	$OMe^- \rightarrow Cu$
378 (3435)	462 (3310)	451 (2140)	373 (2830)	475 (2334)	378 (3555)	378 (3328)	$OPh^- \rightarrow Cu$
					335 (2676)	335 (2216)	$RCOO^- \rightarrow Cu$
	368 (2601)[14]						$N_3^- \rightarrow Cu$[14]
			d–d Bands				
635 (180)	655 (440)	670 (240)	632	680 (524)	630 (228)	625 (162)	
			Solid-State (Nujol Mull) Spectra				
					446 (br)	450 (br)	
					668 (w, br)	685 (w, br)	

[a] λ in nm (ε in M^{-1} cm^{-1}); R = CH_3COO^- (VII), $C_6H_5COO^-$ (VI); br = broad peak, w = weak peak.

tablished for a number of cases.[32] The evidence for the monoatomic bridging in compounds VI and VII further comes from the observation of a band at 378 nm, which we assign to phenolate-to-copper LMCT transitions by analogy to the case for complex I. If acetate and benzoate would have bridged between the two copper atoms via the two different oxygens of a carboxylate group to form a Cu–O–C(R)–O–Cu bridge, we would have expected an opening of the Cu–O1–Cu angle, which in turn would have shifted the 378-nm band to lower energy as in the case of compounds III and V. Carboxylate bridging (μ-1,3) to two Cu(II) ions appears not to contribute any CT features to the electronic spectra of their dinuclear complexes.[23,26]

It is interesting to note that the solid-state spectra for the carboxylate compounds VI and VII are considerably different from the solution-state spectra (Table IX) whereas the solid-state spectra for compounds I–V match their solution spectra. The solids VI and VII do not possess the 378-nm absorption, but instead both complexes show a broad band centered at 450 nm, similar to the case for complexes II, III, and V, which have a larger Cu–O1–Cu bridging angle. Thus, we suggest that, in the solid-state structure of VI (X = benzoate) and VII (X = acetate), the bridging may occur through different oxygen atoms (i.e. μ-acetate-*O,O′*) of the carboxylate ligand as is found in the closely related complexes (μ-acetato-*O,O′*)[2,6-bis(bis(2-(1-pyrazolyl)ethyl)amino)-*p*-cresolato]dicopper(II) diperchlorate–acetone, $[Cu_2(bpeac)(AcO)][ClO_4]_2 \cdot CH_3COCH_3$,[26] and $[Cu_2(L\text{-}Et)(OAc)][ClO_4]_2$,[25] where the ligand HL-Et is *N,N,N′,N′*-tetrakis(1-ethyl-2-benzimidazolyl)-2-hydroxy-1,3-diaminopropane, as well as in a number of other cases.[33]

This structural assignment is also supported by the position of the IR bands (ν_a(COO) = 1520 and 1540 cm^{-1} (Nujol)) for compounds VI and VII, respectively, in accord with a large body of data on metal–carboxylate complexes.[32,37] The observed room-temperature magnetic moment of 1.56 μ_B/Cu for VII also is suggestive of a bridged carboxylate structure since this corresponds to a −2*J* value of ca. −200 cm^{-1},[39] which is in line with (a) the trend observed for −2*J* in complexes I–V and (b) the expected Cu···Cu distance for a bridged carboxylate (greater than 3.3 Å) in this ligand system.[25,26]

Conclusions

Compounds I–VII have been examined as structural biomimics for the previously proposed[6] dicopper(II) sites in met-hemocyanin protein derivatives. The two cupric atoms are bridged by an endogenous phenolate oxygen atom, modeling a proposed endogenous bridging ligand in the proteins.[6] Both of the dinuclear copper atoms, in each compound, exist in tetragonal or distorted

(32) Costes, J.-P.; Dahan, F.; Laurent, J.-P. *Inorg. Chem.* **1985**, *24*, 1018–1022 and references therein.

(33) (a) Lippard, S. J.; Davis, W. M. *Inorg. Chem.* **1985**, *24*, 3688–3691. (b) Van Niekerk, J. H.; Schoenig, F. R. L. *Acta Crystallogr.* **1953**, *6*, 227. (c) DeMeester, P.; Fletcher, S. R.; Skapski, A. C. *J. Chem. Soc., Dalton Trans.* **1973**, 2575.

tetragonal environments. We observe that the exogenous bridging ligand structurally has some effect on the overall copper coordination geometry. The exogenous bridge was found to primarily influence the copper–copper separation, the Cu–$O_{phenolate}$–Cu bridging angle, and the magnetic coupling between Cu(II) ions, while a larger X bridging atom does force the coordination geometry of Cu(II) to deviate from square-based-pyramidal geometry (Table VIII). The latter is also reflected in a general shifting to lower energy of both the $PhO^- \rightarrow$ Cu(II) LMCT band and the d–d envelope (Table IX) as X changes from OR^- to N_3^- to halide. In the proteins it is believed that the two copper atoms are separated by ca. 3.6 Å in oxy- and met-hemocyanin derivatives.[1,2,34] while in the dinuclear compounds I–V the Cu···Cu separation varies between 3.082 and 3.348 Å (Table VIII). There is an apparent preference for monoatomic bridging with shorter Cu···Cu separations (<3.4 Å), although complexes VI and VII may have bridging distances approaching 3.6 Å as solid materials.

As indicated, the spectral properties of complexes I–VII exhibit some dependence on structure, which is dependent on the bridging group X. Magnetochemical properties also vary systematically with structure. While we and others have made considerable progress in establishing structural and spectral correlations in ligand-bridged dinuclear Cu(II) compounds, further investigations are clearly required.

Acknowledgment. We thank the National Institutes of Health (K.D.K., Grant Nos. GM 28962 and GM 34909) and the National Science Foundation (E.S., Grant Nos. CHE83-00516 and CHE83-11449) for support of this research.

Supplementary Material Available: Listings of bond lengths, bond angles, anisotropic temperature factors, and hydrogen coordinates and temperature factors for compounds III (Tables XI–XIV), IV (Tables XVI–XIX), and V (Tables XXI–XXIV) and experimental plots of μ_{eff} and χ vs. $T(k)$ for complexes I–II and V (28 pages); listings of structure factors for complexes III–V (Tables X, XV, and XX) (45 pages). Ordering information is given on any current masthead page.

(34) Spiro, T. G.; Woolery, G. L.; Brown, J. M.; Powers, L.; Winkler, M. E.; Solomon, E. I. In ref 3, pp 23–42.
(35) (a) O'Connor, C. J.; Sinn, E.; Cukauskas, E. J.; Deaver, B. S. *Inorg. Chim. Acta* **1979**, *32*, 29. (b) O'Connor, C. J.; Sinn, E.; Deaver, B. S. *J. Chem. Phys.* **1979**, *70*, 5161. (c) Sinn, E. In *Biological and Inorganic Copper Chemistry*; Karlin, K. D., Zubieta, J., Eds.; Adenine: Guilderland, NY, 1986; Vol. 2, pp 195–220, and references cited therein.
(36) Pyrz, J. W.; Karlin, K. D.; Sorrell, T. N.; Vogel, G. C.; Que, L., Jr. *Inorg. Chem.* **1984**, *23*, 4581.
(37) (a) Armstrong, W. H.; Spool, A.; Papaefthymiou, G. C.; Frankel, R. B.; Lippard, S. J. *J. Am. Chem. Soc.* **1984**, *106*, 3653–3667. (b) Deacon, G. B.; Phillips, R. J. *Coord. Chem. Rev.* **1980**, *33*, 227–250. (c) Nakamoto, K. *Infrared and Raman Spectra of Inorganic and Coordination Compounds*, 4th ed.; Wiley: New York, 1986; pp 231–232.
(38) Thompson, L. K.; Ramaswamy, B. S. *Inorg. Chem.* **1986**, *25*, 2664–2665.
(39) Kahn, O.; Sikorav, S.; Gouteron, J.; Jeannin, S.; Jeannin, Y. *Inorg. Chem.* **1983**, *22*, 2877.
(40) (a) Hatfield, W. E. *Comments Inorg. Chem.* **1981**, *1*, 105–121. (b) Hatfield, W. E. *Inorg. Chem.* **1983**, *22*, 833–837.

Contribution from Department of Chemistry II, Faculty of Science, Hokkaido University, Sapporo 060, Japan

Photoirradiated and γ-Ray-Irradiated Reactions of Manganese(III, IV, V) Tetraphenylporphyrins in 2-Methyltetrahydrofuran. Reactions of Azidomanganese(III) Porphyrin

Takashi Jin, Toru Suzuki, Taira Imamura,* and Masatoshi Fujimoto*

Received February 12, 1986

Manganese(III, IV) tetraphenylporphyrins $Mn^{III}(TPP)X$ (TPP = 5,10,15,20-tetraphenylporphinato; X = I, Br, Cl, N_3, NCS, OAc) and $Mn^{IV}(TPP)(OCH_3)_2$ in 2-methyltetrahydrofuran (MeTHF) at room temperature were reduced to yield $Mn^{II}(TPP)$ by photoirradiation with visible light (440–750 nm) or by γ-ray irradiation. The photoirradiation of $Mn^{III}(TPP)N_3$ in the rigid matrix at 77 K affords $Mn^{V}(TPP)N$. Photochemically stable $Mn^{V}(TPP)N$ was reduced to $Mn^{II}(TPP)$ by γ-irradiation at room temperature. γ-Irradiation of MeTHF solutions of $Mn^{III}(TPP)X$ at 77 K causes one-electron reduction to form the constrained complexes $[Mn^{II}(TPP)X]^-$. Warming the matrices after γ-irradiation formed $Mn^{II}(TPP)$, liberating ligand X^-. The near-infrared bands of $Mn^{III}(TPP)X$ red shift along with the shifts of the bands in the visible region by varying the ligand X. The characteristic bands of the constrained complex $[Mn^{II}(TPP)X]^-$ in the near-infrared region red shift in the order X = Cl > Br > I. The photoirradiation of $Cr^{III}(TPP)N_3$ with visible light affords $Cr^{V}(TPP)N$ at room temperature and at 77 K.

Introduction

Manganese porphyrins have been of continuous interest in the last two decades because of their versatile characteristic behavior in solution: feasible formation of dioxygen complexes,[1,2] photolytic redox reactions,[3] dependency of redox potential on a coordinated monoanion ligand,[4] and electronic spectra of manganese(III) porphyrins.[5,6] Recent syntheses and/or characterization of several high-valent manganese(IV, V) porphyrins,[7,8] including nitridomanganese(V) porphyrins,[9–11] offer much information on synthetic

(1) (a) Hoffman, B. M.; Weschler, C. J.; Basolo, F. *J. Am. Chem. Soc.* **1976**, *98*, 5473. (b) Weschler, C. J.; Hoffman, B. M.; Basolo, F. *J. Am. Chem. Soc.* **1975**, *97*, 5278.
(2) Gonzalez, B.; Kouba, J.; Yee, S.; Reed, C. A.; Kirner, J.; Scheidt, W. R. *J. Am. Chem. Soc.* **1975**, *97*, 3247.
(3) (a) Ellul, H.; Harriman, A.; Richoux, M.-C. *J. Chem. Soc., Dalton Trans.* **1985**, 503. (b) Carnieri, N.; Harriman, A.; Porter, G. *J. Chem. Soc., Dalton Trans.* **1982**, 931, 1231. (c) Engelsma, G.; Yamamoto, A.; Markham, E.; Calvin, M. *J. Phys. Chem.* **1962**, *66*, 2517.
(4) Kelly, S. L.; Kadish, K. M. *Inorg. Chem.* **1982**, *21*, 3631.
(5) (a) Boucher, L. J. *Coord. Chem. Rev.* **1972**, *7*, 289. (b) Boucher, L. J. *J. Am. Chem. Soc.* **1968**, *90*, 6640; **1970**, *92*, 2725.
(6) Boucher, L. J. *Ann. N.Y. Acad. Sci.* **1973**, *206*, 409.
(7) (a) Willner, I.; Otvos, J. W.; Calvin, M. *J. Chem. Soc., Chem. Commun.* **1980**, 964. (b) Schardt, B. C.; Hollander, F.; Hill, C. L. *J. Chem. Soc., Chem. Commun.* **1981**, 765; *J. Am. Chem. Soc.* **1982**, *104*, 3964. (c) Jasinsky, J. P.; Holt, S. L. *Inorg. Chem.* **1975**, *14*, 1267. (d) Camenzind, M. J.; Hollander, F. J.; Hill, C. L. *Inorg. Chem.* **1983**, *22*, 3776. (e) Birchall, T.; Smegal, J. A.; Hill, C. L. *Inorg. Chem.* **1984**, *23*, 1910.
(8) Camenzind, M. J.; Hollander, F. J.; Hill, C. L. *Inorg. Chem.* **1982**, *21*, 4301.
(9) Groves, J. T.; Takahashi, T. *J. Am. Chem. Soc.* **1983**, *105*, 2074.
(10) Buchler, J. W.; Dreher, C.; Lay, K. L. *Z. Naturforsch., B: Anorg. Chem., Org. Chem.* **1982**, *37B*, 1155.

0020-1669/87/1326-1280$01.50/0